* Scattering of Light on Particulate media
* elastic independent isotropic
* inelastic dependent an isotropic

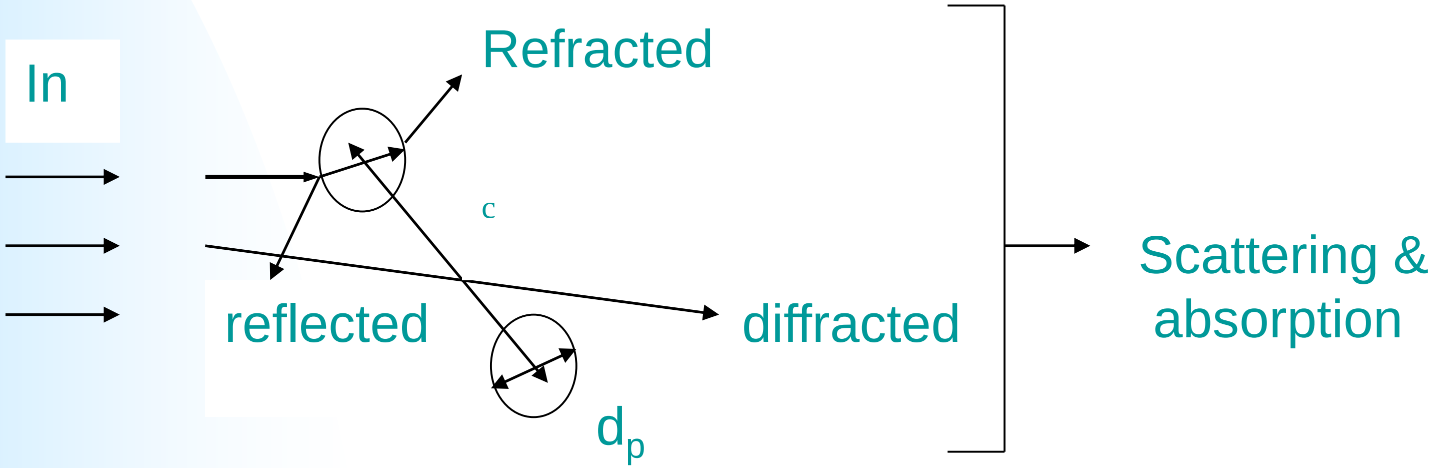

* blue sky, red sunset, rainbow, etc
smog visibility

- **function of particle shape, material of particle (complex index of refraction *m=n-ik*), relative size compared to wavelength of photons, clearance between particles**
- **→ generally assume spherical particles**

(Rayleigh and Mie Scattering), Rayleigh-Debye-Gans theory for non-spherical aggregate

*** independent scattering $c/d_p>4$ or $f_v<0.006$ (volume fraction)**

*** Rayleigh scattering : small particle (Lord Rayleigh(1871))**

$$\frac{\pi d_p}{\lambda} < 0.3 \qquad\qquad \frac{\pi d_p}{\lambda} \approx 1$$

Mie Scattering (1908)
(Gustav Mie : German physicist)

Scattered Power $\approx \frac{1}{\lambda^4}$

Absorbed power $\approx \frac{1}{\lambda}$

(shorter wavelength photons scattered dominantly

Blue sky : blue (shorter scattered wavelength)
Scattered into all directions
Red sunset : large wavelength red rays are able to penetrate the atmosphere without attenuation

* Electro-magnetic wave propagation

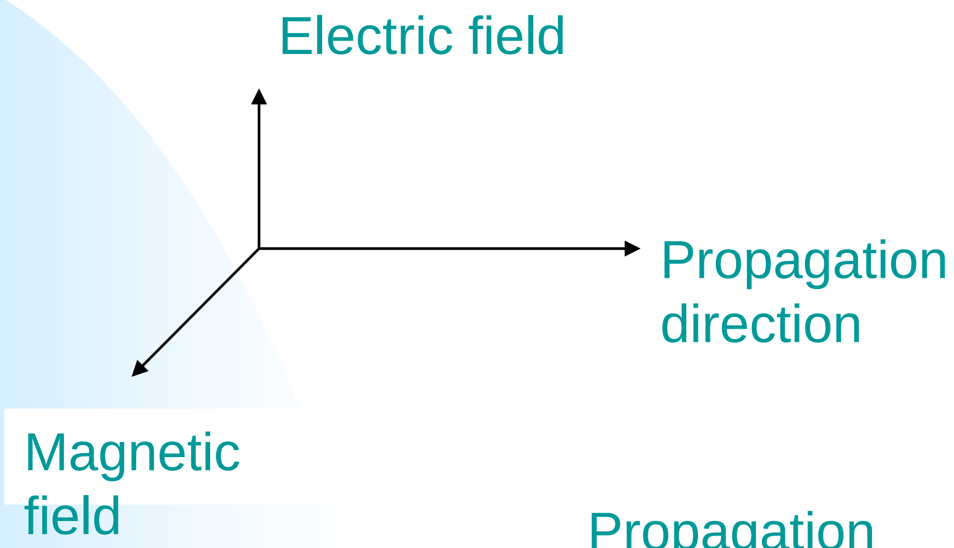

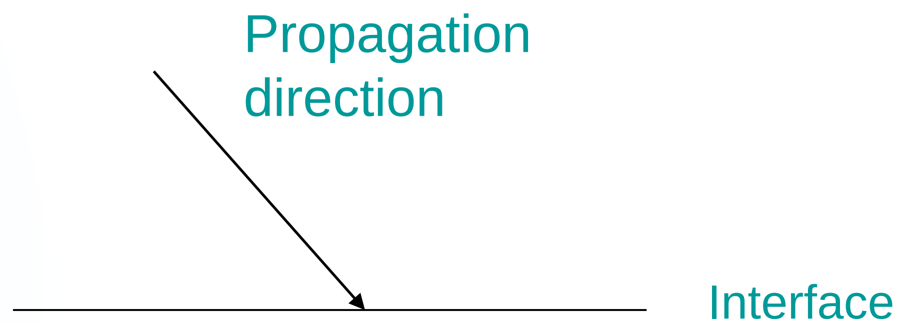

***plane of incidence : plane containing both the normal to interface and incident direction**

***polarization of light**

: horizontally polarized (E-field vector is parallel to the plane of incidence)

: vertically polarized (E-field vector is perpendicular to the plane of incidence)

***Let's consider a single particle illuminated by radiation with incident power per unit area I_0(W/m^2)**

Total scattered power $P_{sca} = C_{sca} I_o$

Total absorbed power $P_{abs} = C_{abs} I_o$

Where C_{sca} and C_{abs} are scattering and absorption cross sections, respectively.

$P_{extinction} = P_{sca} + P_{abs}$
$C_{ext} = C_{sca} + C_{abs}$
Power incident on the particle is $P_{inc}=AI_0$

Where A is the cross sectional area of particle

$$\therefore \frac{P_{abs}}{P_{inc}} = \frac{C_{abs}}{A} = Q_{abs}$$ **: absorption efficiency factor**

$$\therefore \frac{P_{sca}}{P_{inc}} = \frac{C_{sca}}{A} = Q_{sca}$$ **: scattering efficiency factor**

For an aerosol consisting of polydisperse particles effective scattering area

$$= dV\int_0^\infty C_{sca,\lambda}(d_p)dN(d_p)$$

$dN(d_p)$: #/cm^3
between dp and $d_p+dd_p = n(d_p)dd_p$
effective scattering area per unit volume
= scattering coefficient [1/m]

$$\sigma_{s\lambda} = \int_0^\infty C_{sca,\lambda}(dp)dN(dp)$$

if monodisperse

$$\sigma_{s\lambda} = C_{sca,\lambda}N$$

$$I = I_0 \exp(-(\sigma_{s\lambda} + \alpha_\lambda)x)$$

$$dI = -I \frac{C_{sca}}{A}$$

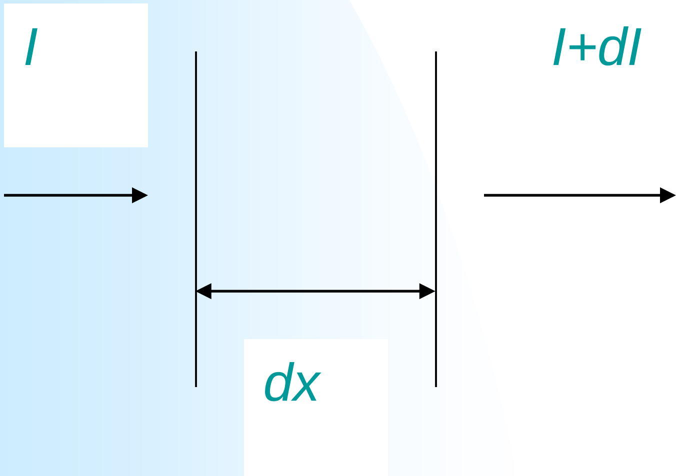

$$dI = -I \frac{effective\ \ scattering\ \ area}{A} = -I \frac{dV\sigma_{s\lambda}}{A}$$

$$= -Idx\sigma_{s\lambda}$$

$$\frac{dI}{I} = -\sigma_{s\lambda} dx$$

$$\therefore \frac{I}{I_o} = \exp(-\sigma_{s\lambda} x)$$

•Rayleigh scattering

$$x = \frac{\pi d_p}{\lambda} \rightarrow 0$$

$$Q_{sca} = \frac{8}{3}\left|\frac{m^2-1}{m^2+2}\right|^2 x^4 \approx \frac{1}{\lambda^4}$$

$$Q_{ext} = -4x\,\mathrm{Im}\{\frac{m^2-1}{m^2+2}\} \approx Q_{abs}$$

$$C_{ext} = \pi\frac{d_p^{\,2}}{4}Q_{ext} \qquad \overline{C_{ext}} = \int C_{ext}\,p(d_p)\,dd_p$$

$$\sigma_{ext} = \int_0^\infty C_{ext}\,n(v)\,dv = -\frac{6\pi}{\lambda} f_v\,\mathrm{Im}\{\frac{m^2-1}{m^2+2}\}$$

→ only depends on volume fraction not on particle size distribution

f_v **= volume fraction**

$$\frac{I_{ext}}{I_o} = \exp(-\int\sigma_{ext}\,ds)$$

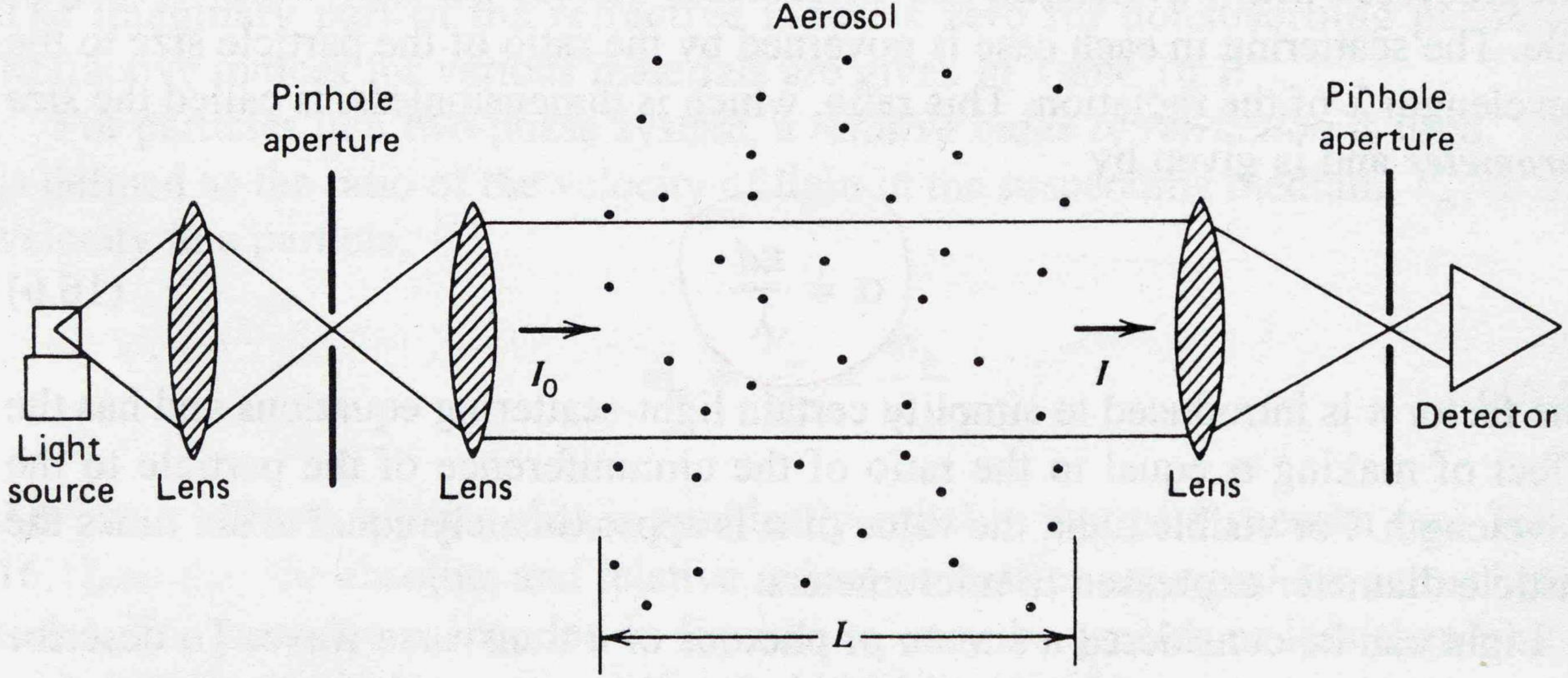

FIGURE 16.1 Schematic diagram of an extinction-measuring apparatus.

Extinction-Scattering method for small particles

Rayleigh scattering & extinction

$$C_{ext} = -4\frac{2\pi^2 a^3}{\lambda}\,\mathrm{Im}\{\frac{m^2-1}{m^2+2}\}$$

$$\overline{C_{ext}} = \int_0^\infty -\frac{\pi^2 d_p^{\,3}}{N\lambda}\frac{1}{\sqrt{2\pi}\ln\sigma_g d_p}\exp\left(-\frac{(\ln {d_p}/{d_g})^2}{\ln\sigma_g}\right)dd_p \times \mathrm{Im}\{\frac{m^2-1}{m^2+2}\}$$

$$= \frac{\pi^2}{\lambda} d_{\bar{m}}^3 E(\tilde{m})$$

$d_{\bar{m}}$: diameter of average volume

$$\therefore d_{\bar{m}}^3 = \frac{\lambda}{\pi^2}\frac{\overline{C_{ext}}}{E(\tilde{m})}$$

$$f_v = \frac{1}{6}\pi d_m^3 N = \frac{\lambda}{6\pi}\frac{1}{E(\tilde{m})}\overline{C_{ext}}N$$

Since $\overline{C_{ext}}N = K_{ext}$, we can measure f_v from K_{ext}

Differential scattering cross-section for vertically polarized light

$$C_{vv}(\theta) \approx \frac{a^6}{\lambda^4}\left|\frac{m^2-1}{m^2+2}\right|^2$$

$$\overline{C(\theta)_{vv}} = \int_0^\infty C_{vv}(\theta)p(d_p)dd_p = \frac{1}{(2\pi/\lambda)^2}\left(\frac{\pi}{\lambda}\right)^6\frac{M_6}{M_0}F(m) \quad \sim d_p^6$$

$$\frac{M_6}{M_0} = \int_0^\infty d_p{}^6 p(d_p)dd_p$$

$$\overline{C_{ext}} = \frac{\pi^2}{\lambda}\frac{M_3}{M_0}E(m) \quad \sim d_p^3$$

$$\frac{\overline{C_{vv}}}{\overline{C_{ext}}} = \frac{\pi^2}{4\lambda^3}\frac{M_6}{M_3}\frac{F(m)}{E(m)} \quad \sim d_p^3$$

$$\therefore M_6 / M_3 = \left(\frac{\lambda^3}{\pi^3}\right)\left\{4\pi\frac{\overline{C_{vv}}}{\overline{C_{ext}}}\frac{E(m)}{F(m)}\right\}$$

$$\therefore \left(\frac{M_6}{M_3}\right)^{1/3} = \frac{\lambda}{\pi}\left\{4\pi\frac{\overline{C_{vv}}}{\overline{C_{ext}}}\frac{E(m)}{F(m)}\right\}^{\frac{1}{3}}$$

$$d_{p63} = \left(\frac{M_6}{M_3}\right)^{1/3} = \left(\frac{\int d_p{}^6 n(d_p)\,dd_p}{\int d_p{}^3 n(d_p)\,dd_p}\right)^{1/3}$$

If we assume log-normal distribution,

$$\frac{M_0 M_6}{M_3^2} = \{\frac{dp_{63}}{dp_{30}}\}^3 = \exp(9\ln^2\sigma_g)$$

If σ_g is known, then d_{p30} can be determined.

$\sigma_g = 1$ → monodisperse

$\sigma_g \approx 1.36$ → self-preserving

absorbing particle only : carbon soot particle

* Mie Scattering

$$Q_{sca} = \frac{2}{x^2}\sum_{n=1}^{\infty}(2n+1)(|a_n|^2 + |b_n|^2)$$

$$Q_{ext} = \frac{2}{x^2}\sum_{n=1}^{\infty}(2n+1)R(a_n + b_n)$$

$$C_{sca} = \pi \frac{d_p^{\ 2}}{4} Q_{sca} = \int_{4\pi} (differential\ cross\ section)\, d\Omega$$

Consider only vertically polarized comp.→ $C_{vv}(\theta, d_p, m)$

Scattering angle

m=n-*ik*

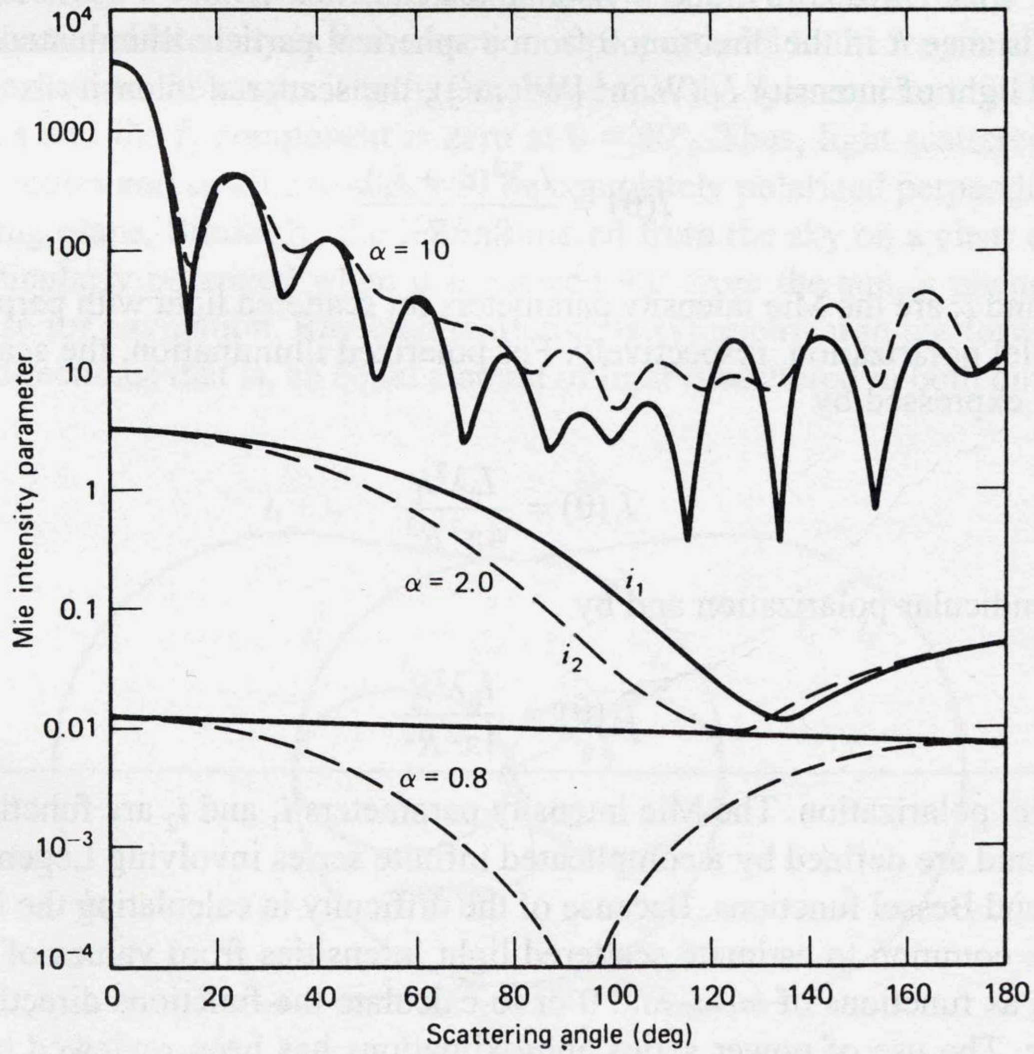

FIGURE 16.8 Mie intensity parameters versus scattering angle for water droplets (m = 1.33) having α = 0.8, 2.0, and 10.0. Solid lines are i_1 and dashed lines are i_2.

We can determine particle size distribution by measuring scattered lights at different angles → angular dissymmetric light scattering method

differential scattering coefficient

$$\sigma_s(\theta) = \int_0^{\infty} C_{vv}(x, \theta, m) n(v) dv$$

Assume independent scattering → or single scattering

* Detected power of scattered light

$$S_{vv}(\theta) = \sigma_s(\theta)\eta\Delta V\Delta\Omega I_{0,vv}$$

$$= \sigma_s(\theta) SR(\theta)$$

$SR(\theta)$ = system response (independent of size distribution or material)

(Example)

$$n(v) = \frac{M_0}{3\sqrt{2\pi}\ln\sigma_g}\exp\left[-\frac{\ln^2(v/v_g)}{18\ln^2\sigma_g}\right]\frac{1}{v}$$

M_0, v_g, σ_g : 3 unknowns

$$SR(\theta)\int_0^\infty C_{vv}(x,\theta)\frac{M_0}{3\sqrt{2\pi}\ln\sigma_g}\exp\left[-\frac{\ln^2(v/v_g)}{18\ln^2\sigma_g}\right]\frac{1}{v}dv$$

$$= S_{vv}(\theta)$$

$$\frac{S_{vv}(\theta_1)}{SR(\theta_1)} = \int_0^\infty C_{vv}(x,\theta_1)\frac{M_0}{3\sqrt{2\pi}\ln\sigma_g}\exp\left[-\frac{\ln^2(v/v_g)}{18\ln^2\sigma_g}\right]\frac{1}{v}dv$$

$$\frac{S_{vv}(\theta_2)}{SR(\theta_2)} = \int_0^\infty C_{vv}(x,\theta_2)\frac{M_0}{3\sqrt{2\pi}\ln\sigma_g}\exp\left[-\frac{\ln^2(v/v_g)}{18\ln^2\sigma_g}\right]\frac{1}{v}dv$$

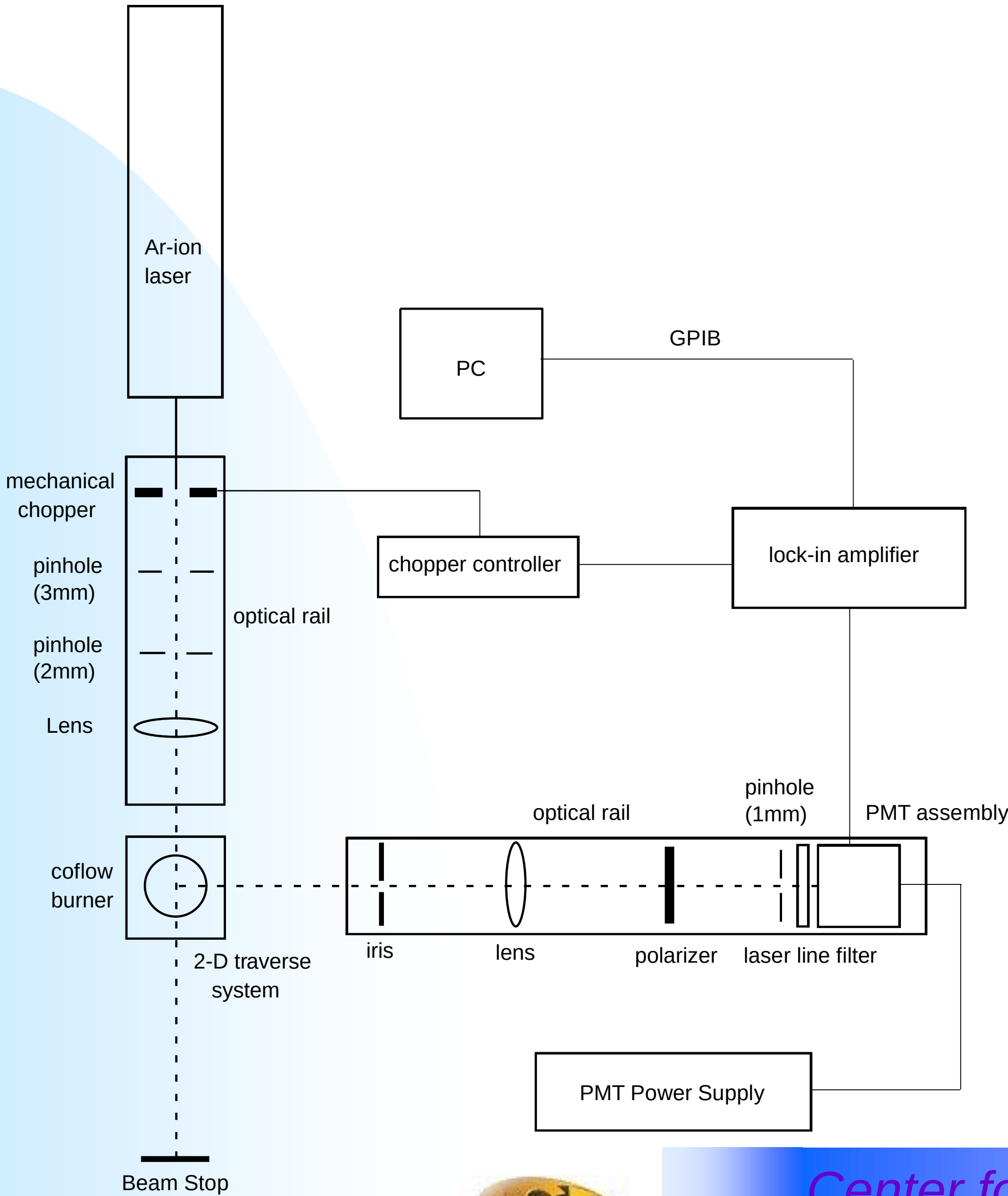
Ar-ion
laser
PC
GPIB
mechanical
chopper
chopper controller
lock-in amplifier
pinhole
(3mm)
optical rail
pinhole
(2mm)
Lens
pinhole
(1mm)
optical rail
PMT assembly
coflow
burner
iris
lens
polarizer
laser line filter
2-D traverse
system
PMT Power Supply
Beam Stop

Optical Particle Counter (OPC):

- measures particle size distribution covering the size range 0.1-5 μm. The aerosol flow should be diluted to make sure that only one particle at a time is illuminated and scatters light to the detector. As each particle passes through the focused light beam, it scatters a pulse of light to the detector, which is converted to an electrical signal. Electronic pulse height (or area) analysis is used to interpret the pulse and direct a count to the proper size channel where the total count is obtained from the accumulated counts in each size channel.

- Optical particle counters are restricted by “coincidence errors” to the measurement of aerosols with relatively low number concentrations usually less than 10(4)/cc. Coincidence errors arise when two or more particles are in the measuring volume simultaneously and causing a spurious signal that leads to an underestimation of the particle number concentration and the overestimation of the particle size.

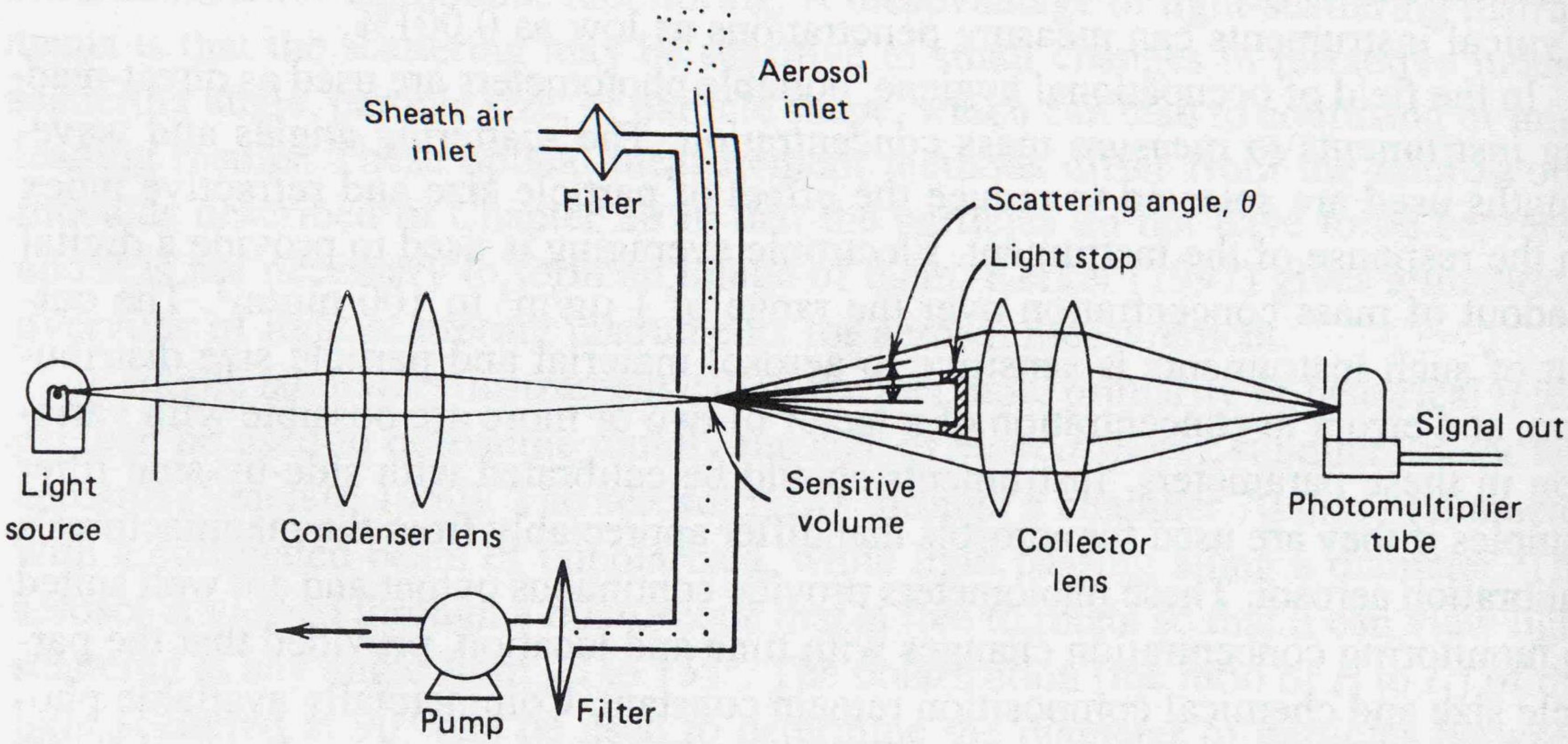

FIGURE 16.15 Diagram of a forward-scattering optical particle counter.

TABLE 16.3 Characteristics of Some Optical Particle Counters

Instrument	Particle Size Range (μm)	Number of Channels	Scattering Angle Range (deg)	Sample Flow Rate (cm^3/min)	Maximum Concentration[a] (cm^{-3})
Climet[b]					
208[c]	0.3–>20	16	15–105	28,000	90
7400	0.1–>0.5	6	15–150	2800	14
7500	0.19–>5.0	6	15–150	28,000	14
Hiac/Royco[d]					
236	0.12–>6.0	16	35–120	280	3000
5100	0.25–>10	6	60–120	28,000	7
PMS, Inc.[e]					
HS-LAS	0.065–1.0	32	35–120	2800	8000
LAS-X	0.09–3	16[f]	35–120	60	17,000
LAS-X	0.12–7.5	16[f]	35–120	280	3000
LPC-525	0.2–>5.0	6	60–120	28,000	3.5

[a]Concentration for 10 % coincidence error.
[b]Climet Instruments Co., Redlands, CA.
[c]White light illumination; all others use laser light.
[d]Hiac/Royco, Menlo Park, CA.
[e]Particle Measuring Systems, Inc., Boulder, CO.
[f]Four ranges with 16 channels each.

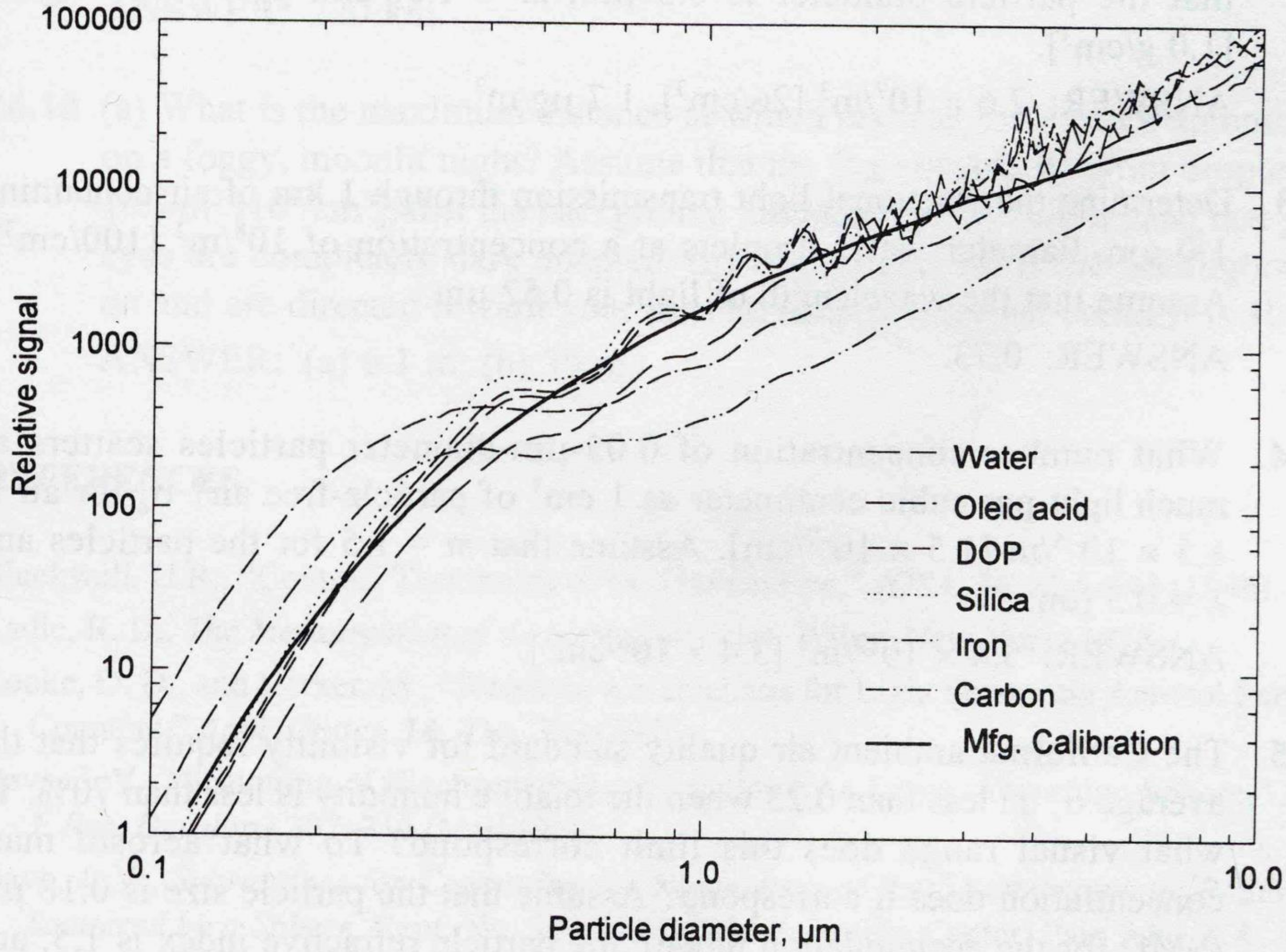

FIGURE 16.16 Calculated response curves for six materials and manufacturer's calibration curve for model LAS-X® (PMS, Inc., Boulder, CO) optical particle counter.

Evolution of size, morphology, and concentration of particles

- **Particle growth**

  : size and morphology change, concentration change

  : spherical, non-spherical

- **Evolution of size distribution of aerosol**
- **What makes the size distribution change?**

- **Convection, diffusion, external force → aerosol transport and migration → concentration change, but size and morphology remain**
- **Collision of Particles**

  : size, morphology and concentration changes
- **Condensation and Evaporation**

  : size change
- **Coalescence of particles**

  : morphology change
- Nucleation

  : generation of particles

Nanoparticle synthesis-Flame Aerosol Synthesis

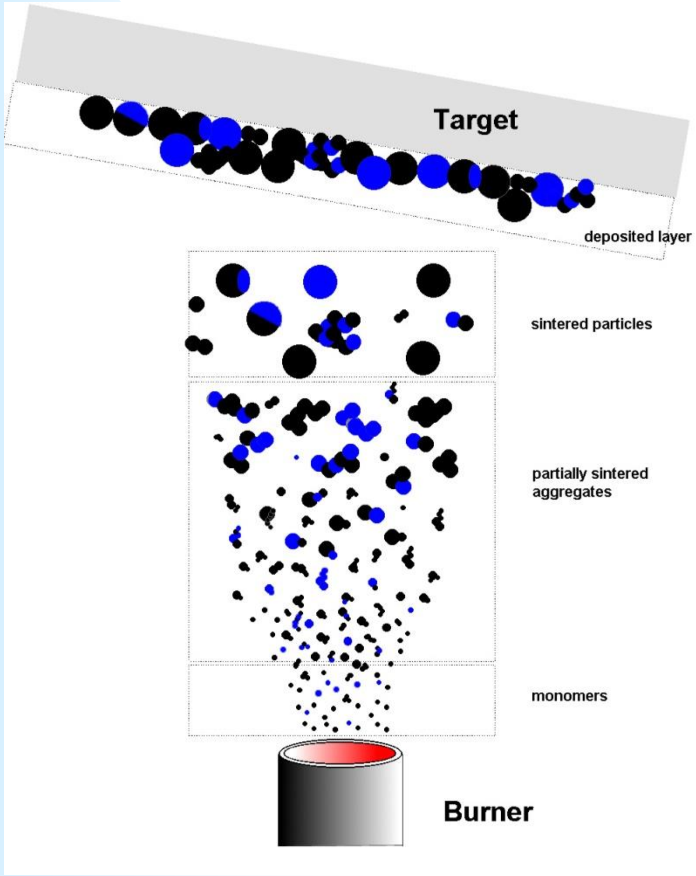

Pro : high purity nanoparticles at high concentrations

Con : difficulty in controlling the growth of nanoparticles : generation of aggregates when nanoparticles are synthesized at high concentrations.

"How can we synthesize small and unagglomerate sphere nanoparticles at high concentrations?"

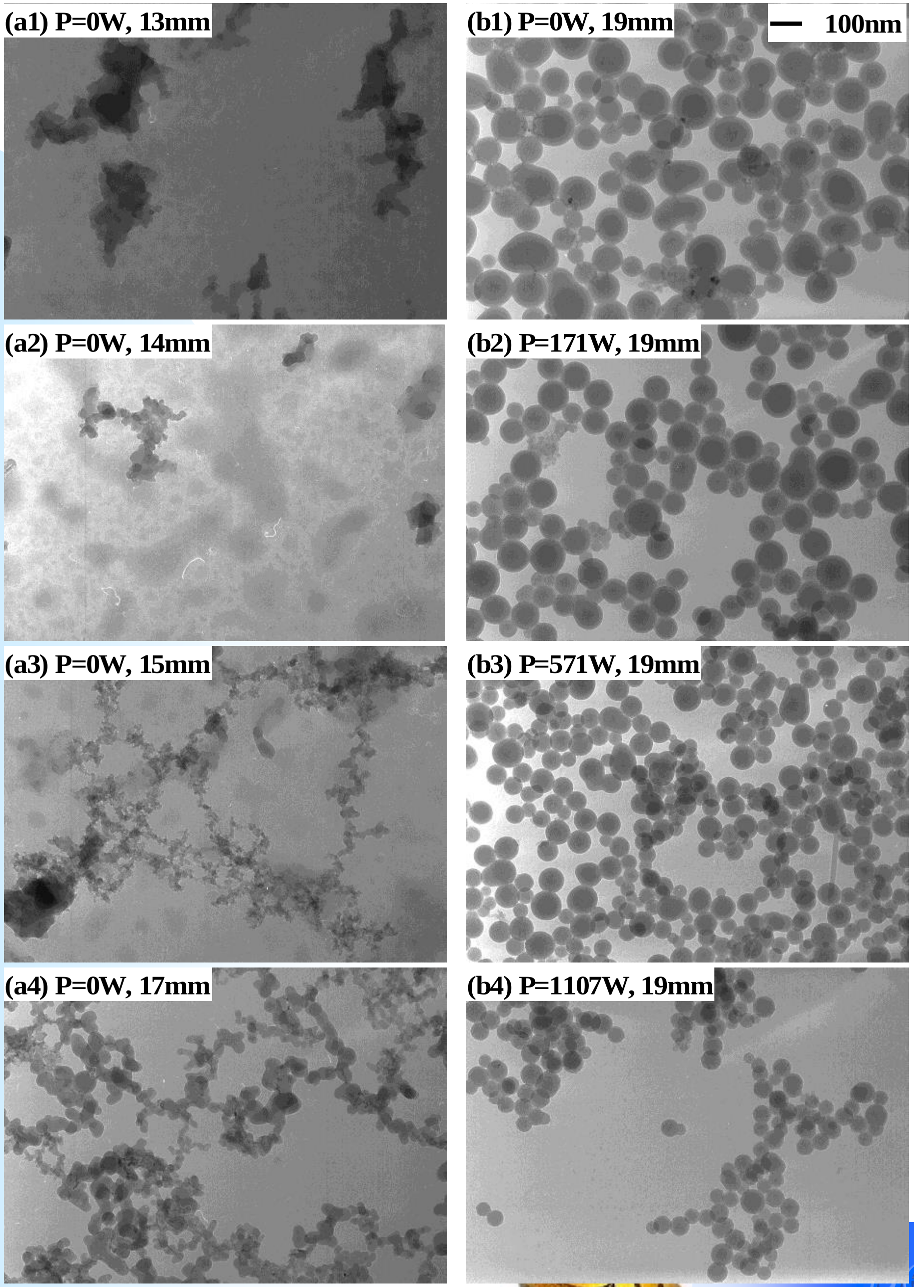

Growth of SiO_2 Particles in a Flame

- **Generation of nanoparticles : Physical or chemical**
  - **Homogeneous nucleation or chemical reactions**
  - **Temperature and concentration fields**
- **Growth of nanoparticles :**
  - **Collision and coalescence (+residence)**
  - **Temperature, concentration and fluid flow fields**
- **Transport of nanoparticles :**
  - **Diffusion, convection and thermophoresis**
  - **Temperature, concentration and fluid flow fields**
- **Deposition of nanoparticles :**
  - **Diffusion and thermophoresis**
  - **Temperature and concentration gradients**

Description the morphology of non-spherical particles;

$$n_p = k_f \left(\frac{R_g}{d_p}\right)^{D_f}$$

(i) Mass fractal dimension, D_f

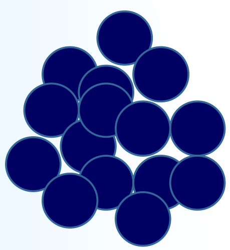

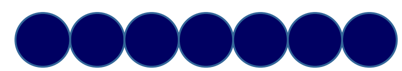

D_f=3: Compact agglomerate structure

D_f =1: Chain-like

Fractal dimension

$$N_p = k_f \left(\frac{R_g}{r_p}\right)^{D_f}$$

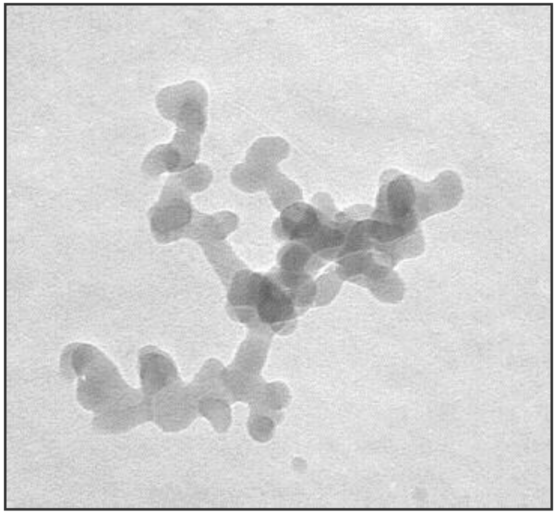

Image processing

N_p : primary particle number per aggregate

$$N_p = \left(\frac{A_a}{A_p}\right)^{1.1}$$

$$A_a = D_{binary}$$

$$A_p = \pi r_p^2$$

R_g : radius of gyration

$$MR_g^2 = \sum_i m_i (\vec{r}_i - \vec{r}_{cm})^2$$

$$D_{binary} R_{g,2}^2 = \sum_i D_{binary,i} (\vec{r}_i - \vec{r}_{cm})^2$$

$$R_g \approx R_{g,2}$$

D_f : fractal dimension

Slope of $\ln(N_p) - \ln(R_g / r_p)$ plot

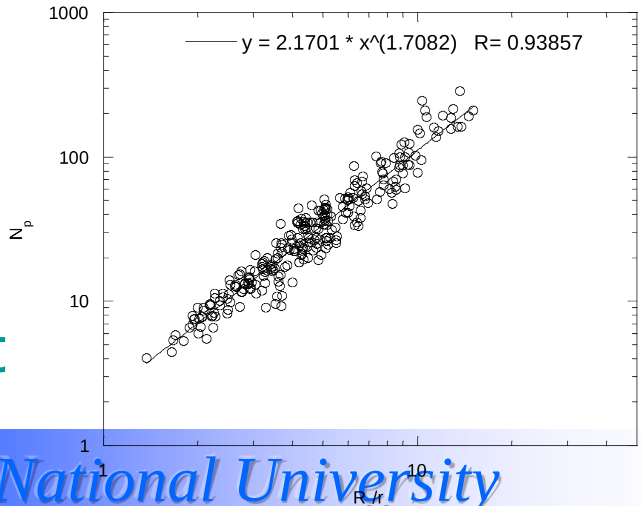

Determination of Size and Morphology

- **Competition between Collision and Coalescence of nanoparticles**
  - **If collision is faster than coalescence, aggregate form**
  - **If coalescence is faster than collision, spherical particle form**

Cho and Choi, 2000, J. Aerosol Sci., 31, 1077

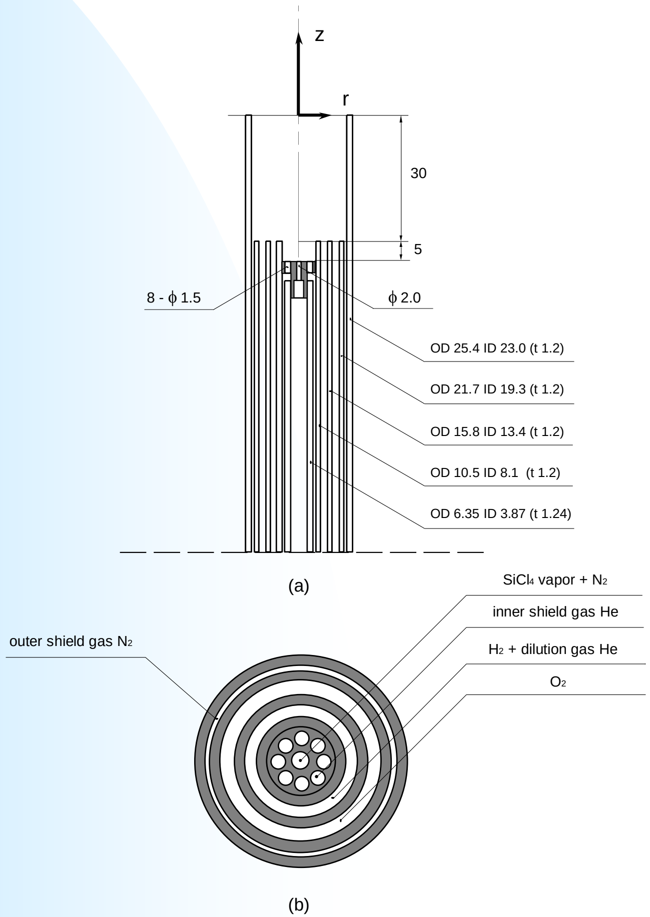

Fig.1 (a) Schematic of a coflow burner and coordinates (unit : mm)
(ID : inside diameter, OD : outside diameter, t : thickness)
(b) Burner exit configuration

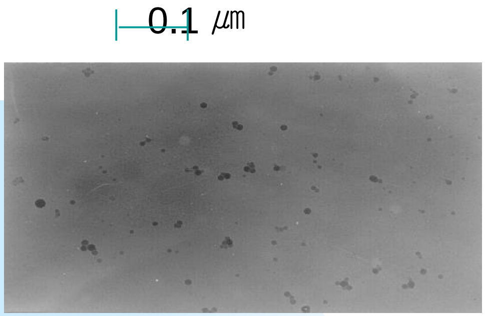

(a) 30 cc/min

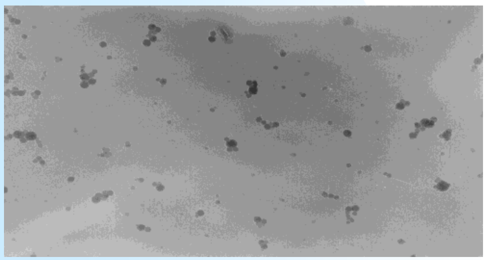

(b) 50 cc/min

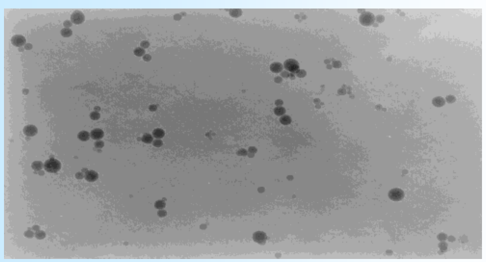

c) 100 cc/min

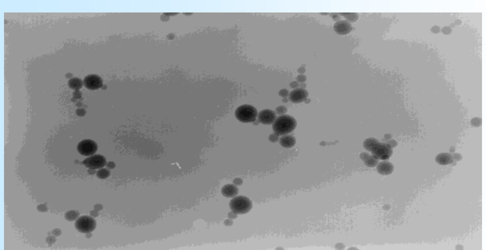

d) 150 cc/min

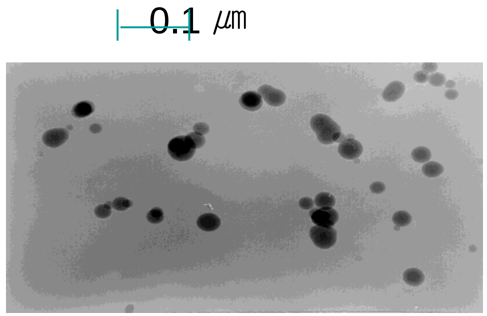

(e) 200 cc/min

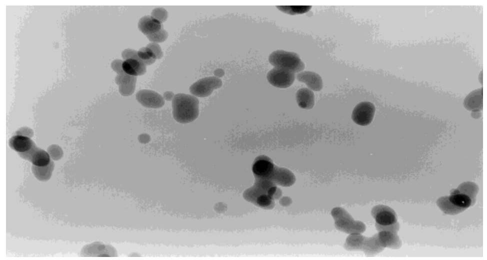

(f) 250 cc/min

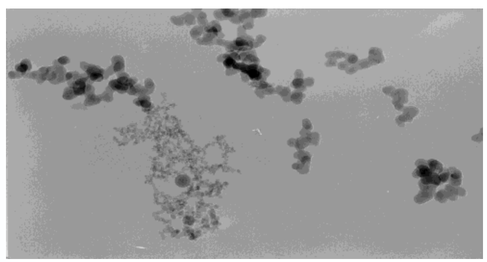

(g) 300 cc/min

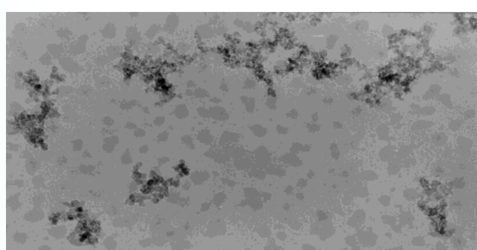

(h) 350 cc/min

Effect of carrier gas flow rates on the morphology of SiO_2 particles in flames (inner shield He 3.0 l/min, H_2 4.0 l/min, dilution He 2.0 l/min, O_2 7.5 l/min, outer shield N_2 7.0 l/min, carrier gas N_2 for $SiCl_4$, r = 0 mm, z = 5 mm)

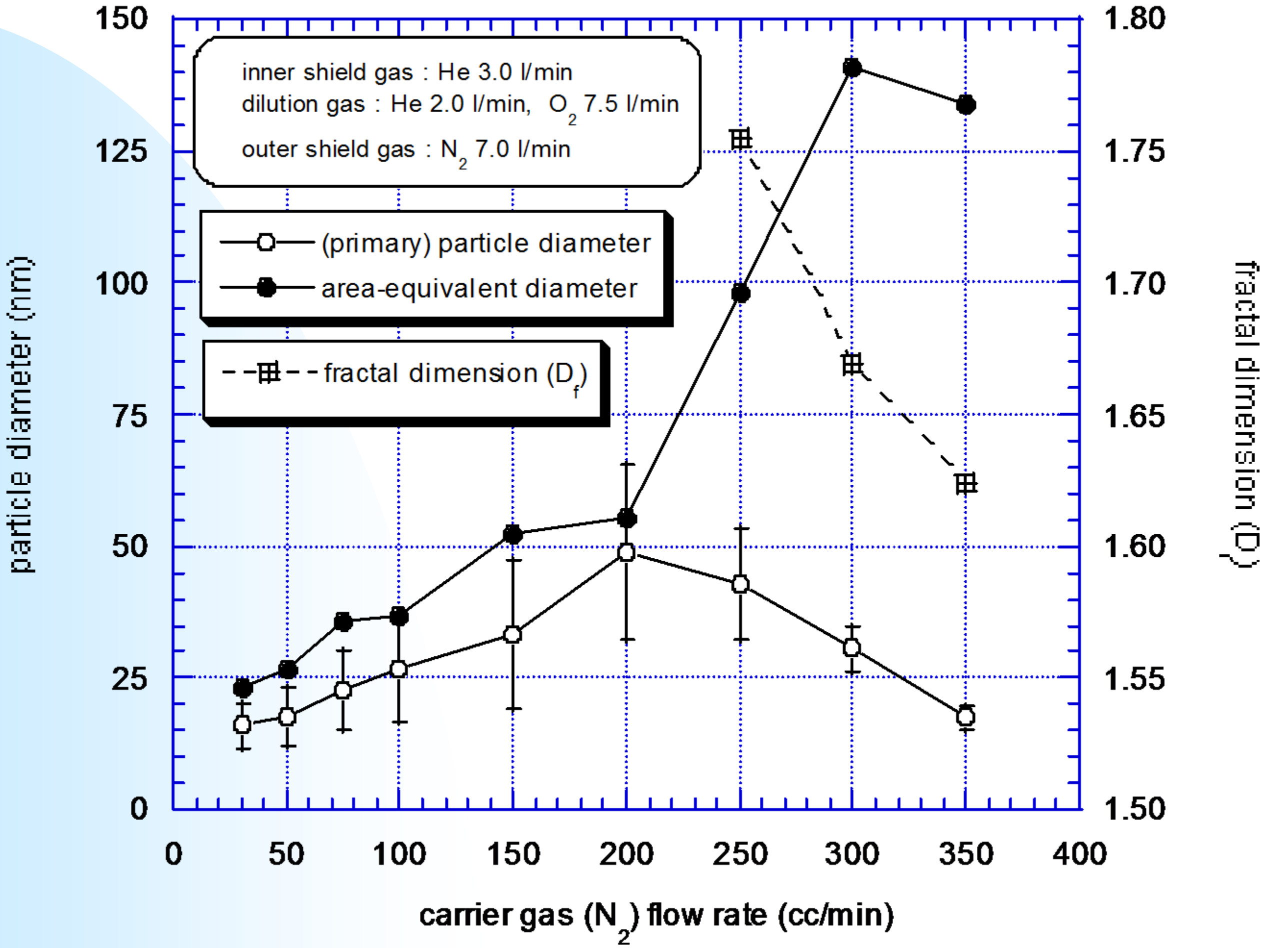

Fig.6 Effect of carrier gas flow rate on particle diameters and fractal dimensions

(H_2 4.0 l/min, r = 0 mm, z = 5 mm, carrier gas N_2)

|—| 0.1 ㎛

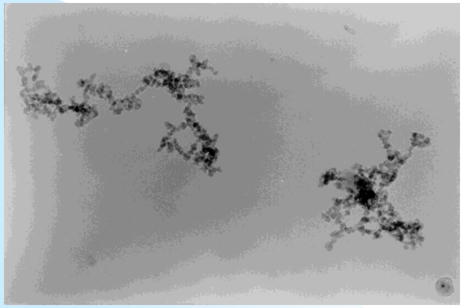

(a) H_2 1.5 l/min,
Q_{vv}= 1.048E-3 ±z3.59%

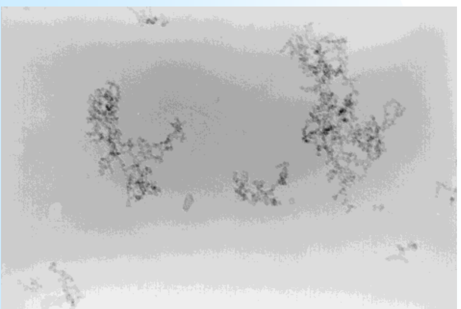

(b) H_2 2.0 l/min,
Q_{vv}= 8.281E-4 ± 4.79%

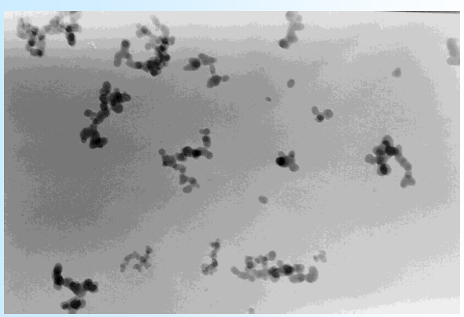

(c) H_2 2.5 l/min, Q sub vv
Q_{vv}= 1.750E-3 ± 5.15%

|—| 0.1 ㎛

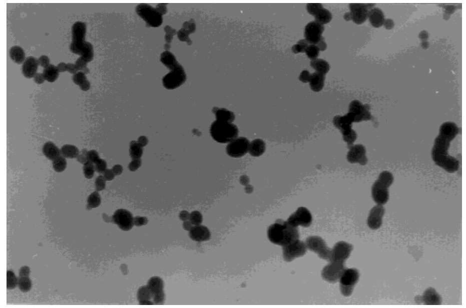

(d) H_2 3.0 l/min,
Q_{vv}= 3.395E-3 ± 4.24%

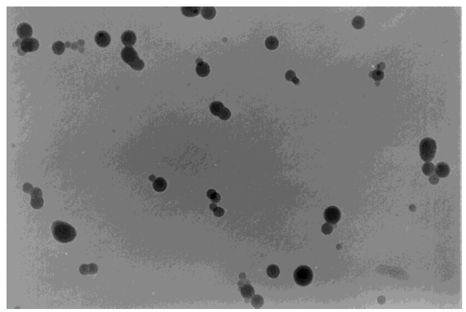

(e) H_2 4.0 l/min,
Q_{vv}= 2.079E-3 ± 5.63%

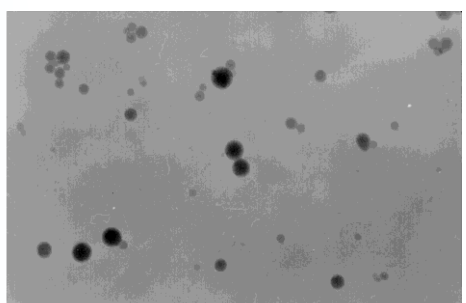

(f) H_2 5.0 l/min, Q sub vv
Q_{vv}= 1.091E-3 ± 7.18%

Effect of H_2 flow rates on the morphology of SiO_2 particles in flames (inner shield He 3.0 l/min, dilution He 2.0 l/min, O_2 7.5 l/min, outer shield N_2 7.0 l/min, carrier gas N_2 50 cc/min for $SiCl_4$, r = 0 mm, z = 30 mm, unit of Q_{vv} : [cm^{-1} sr^{-1}])

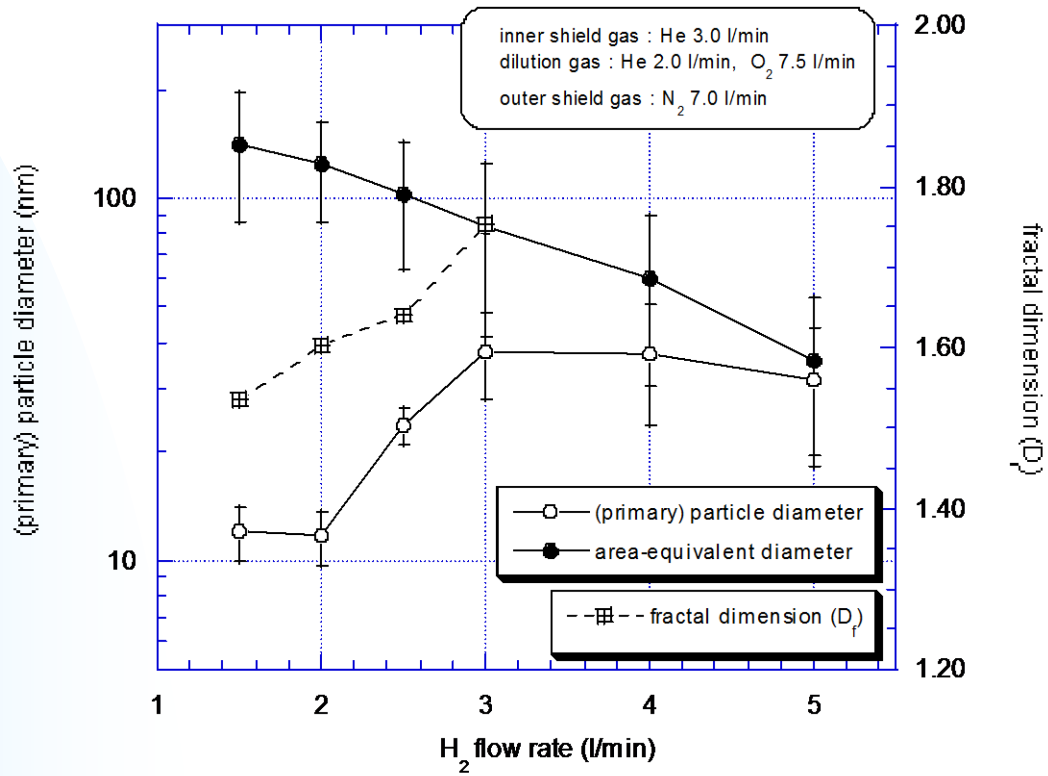

Fig.11 Effect of H_2 flow rates on particle diameters and fractal dimensions

(carrier gas N_2 50 cc/min for $SiCl_4$, r = 0 mm, z = 30 mm)

Present Control Principle

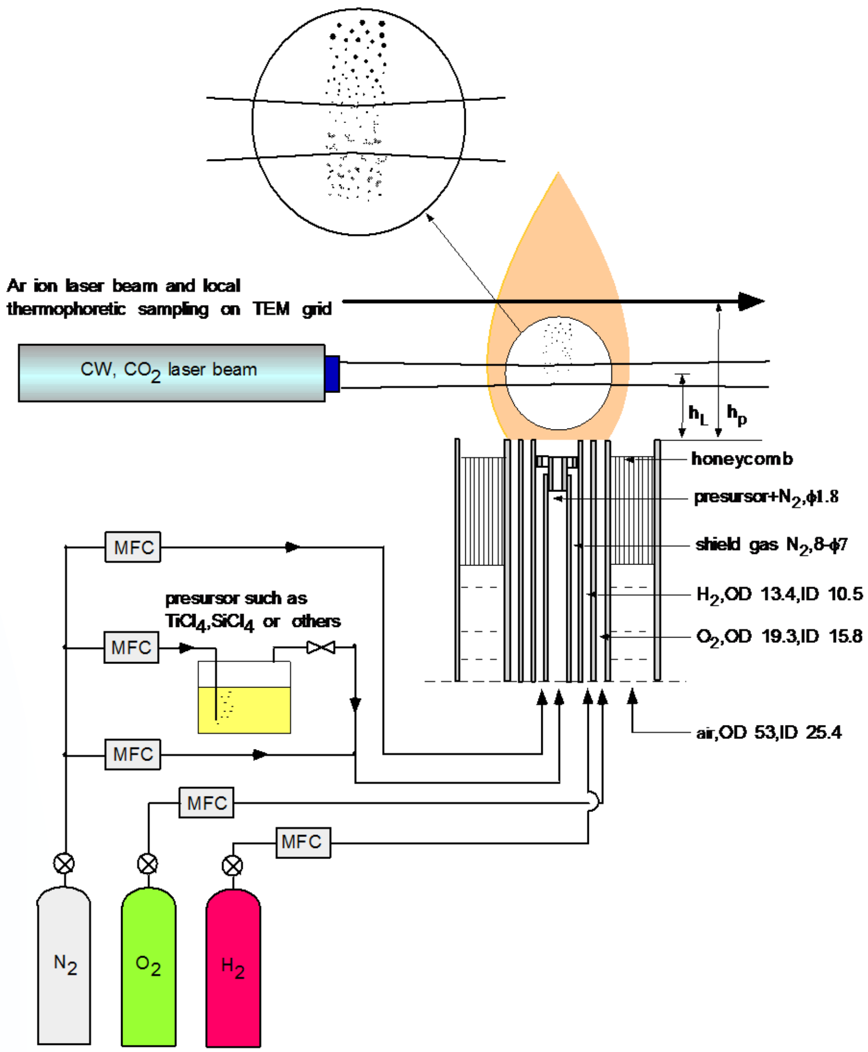

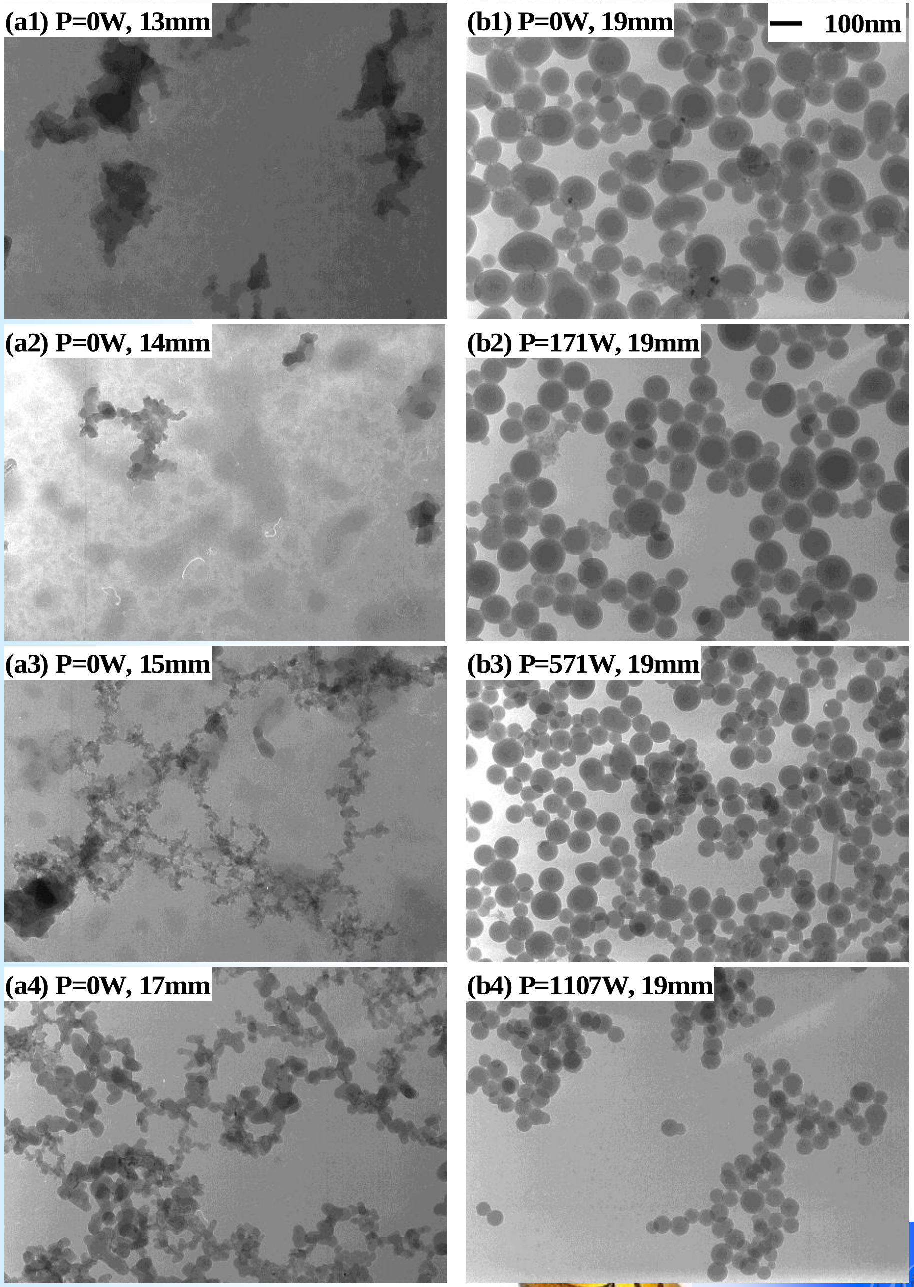

Growth of SiO_2 Particles in a Flame

Aerosol Synthesis of Nanoparticles

- **Nanoparticle grows by two processes : particle collision and coalescence.**

1. If collision is faster than coalescence,

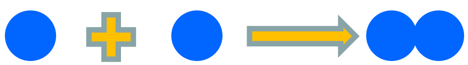

: aggregates form.

2. If coalescence is faster than collision,

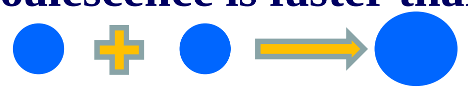

: spheres form.

Collision characteristic time ~ $\frac{1}{\sqrt{T}}$

Coalescence characteristic time ~ $\exp\left(\frac{C}{T}\right)$

➡ **Heat transfer can control the rates of collision and coalescence, then the size and morphology of nanoparticle can be controlled.**

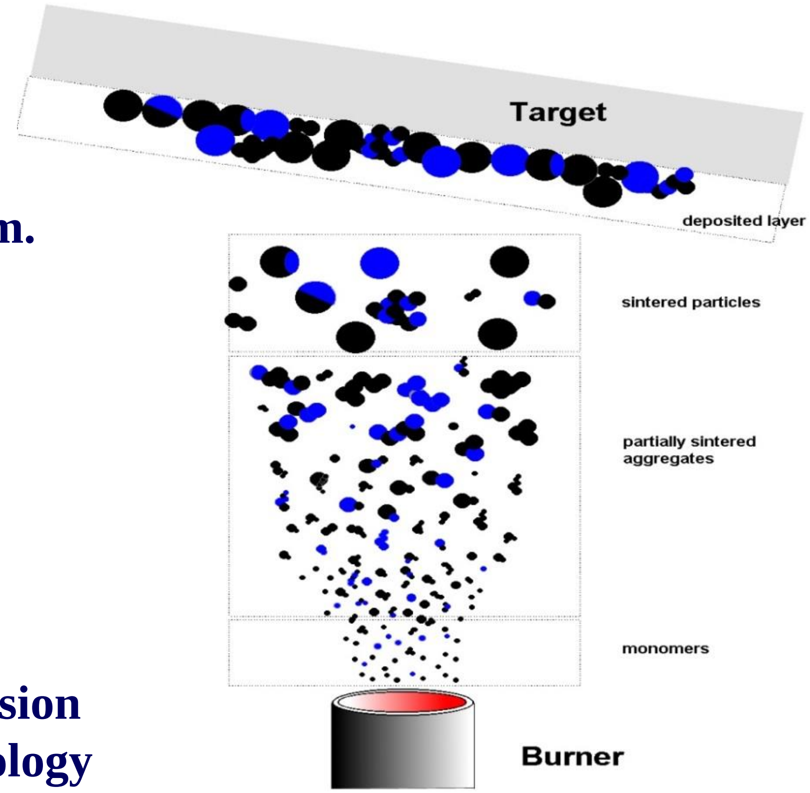

- **Nanoparticle crystallinity can be also controlled by heat transfer.**

Present Control Principle

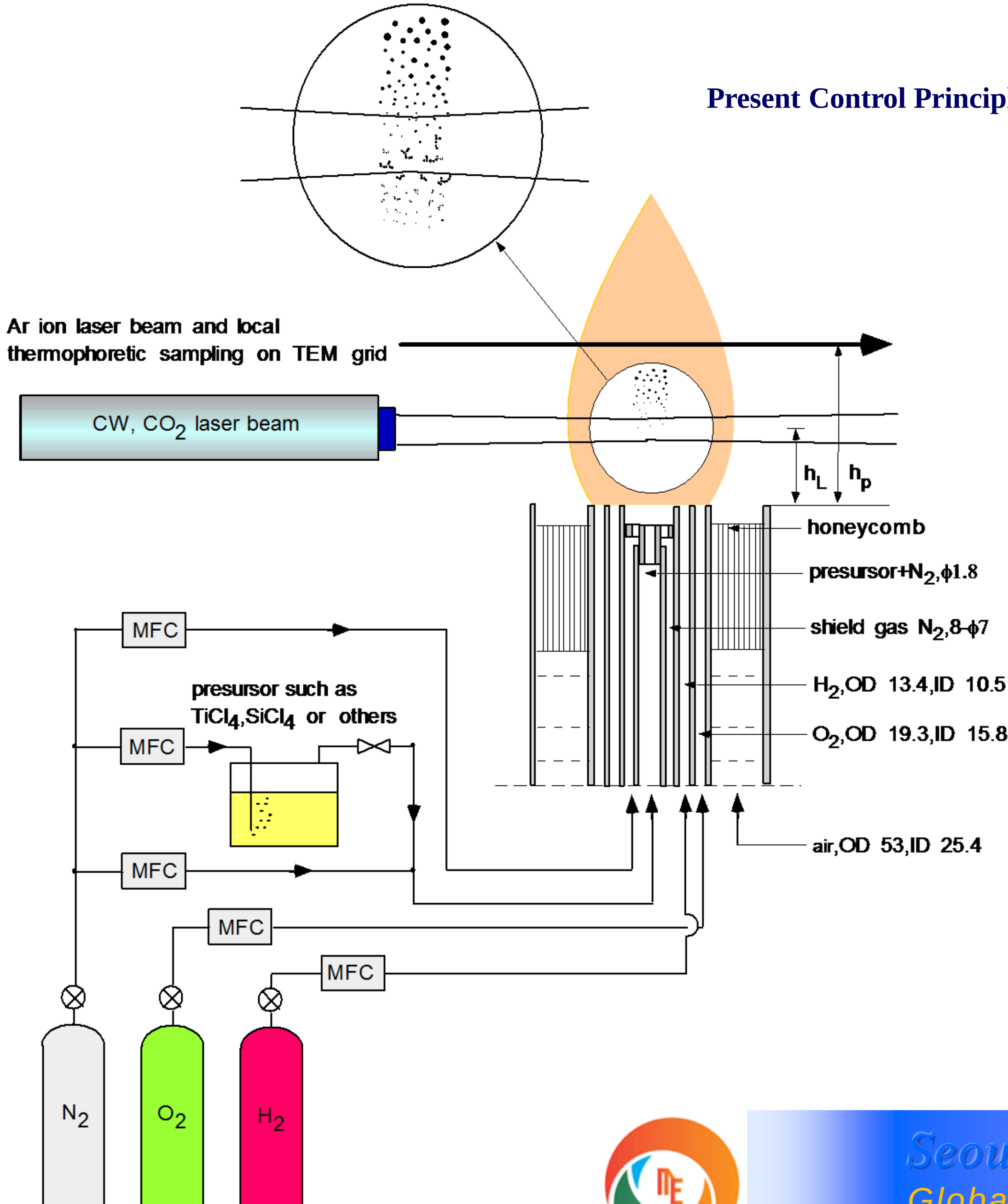

Laser irradiation in a particle generating flame can enhance coalescence by increasing particle temperature.

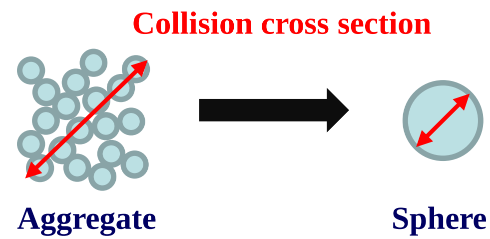

By enhancing coalescence, collision probability can be greatly reduced

➡ **Much smaller and, at the same time, spherical nanoparticles at higher concentrations.**

Apply the Method to Crystalline TiO2

(Lee and Choi, 2002 J. Aerosol Science 33, 1-16)

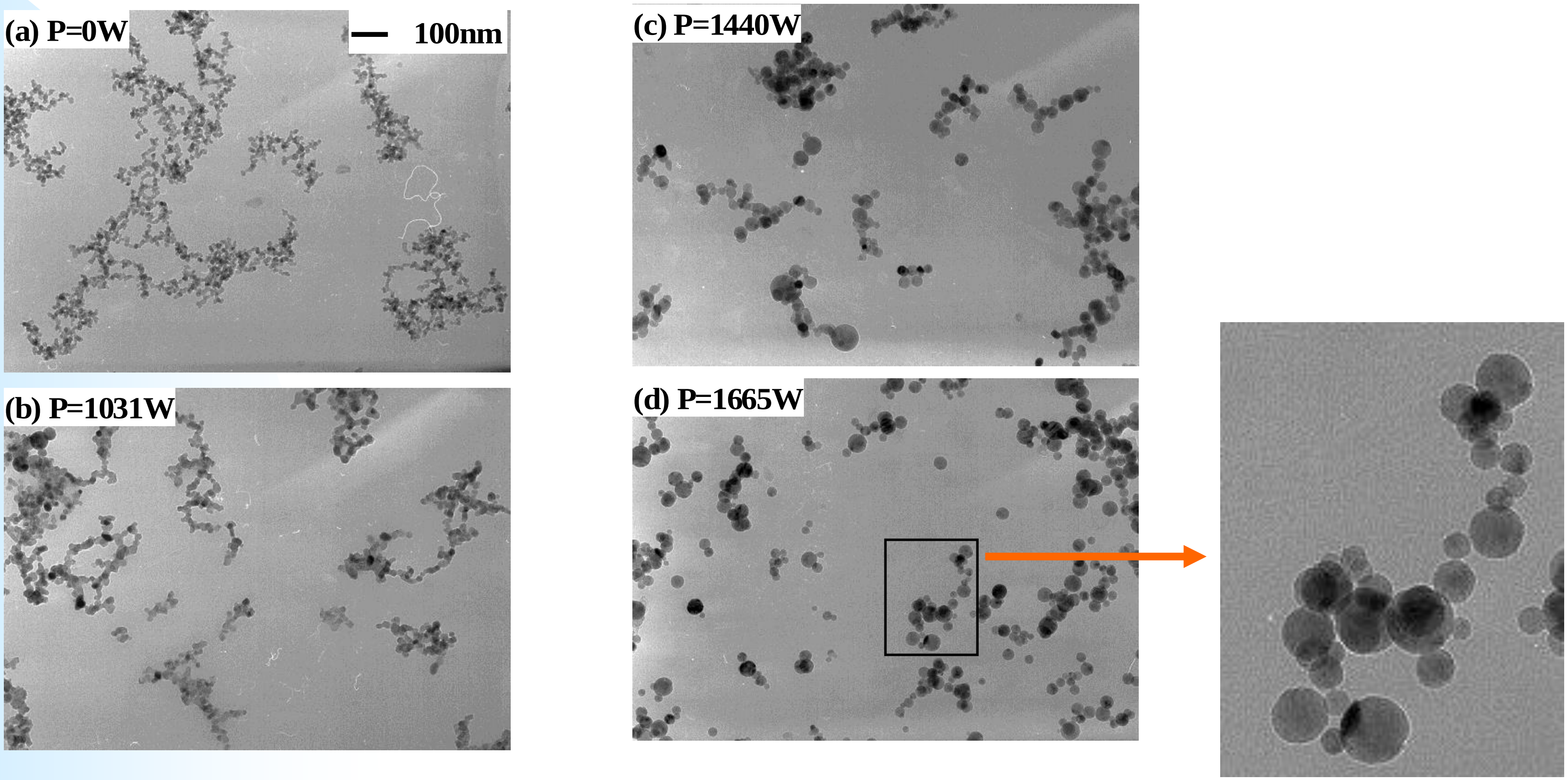

$TiCl_4 = 9.6 \times 10^{-4}$ mol/min

$h_L = 13$ mm

$h_P = 16$ mm

Variations of Size, Number Concentration and Volume Fraction

	P = 0 W	P = 2405 W	Note
d_a (nm)	109.6	20.3	
d_v (nm)	58.7	20.3	Particle volume reduction by 24 times
N (#/cm^3)	1.77×10^9	3.77×10^{10}	Particle number increase by 21 times
f_v	2.71×10^{-7}	2.49×10^{-7}	

d_a : projected area equivalent diameter

d_v : volume equivalent diameter

Transformation of Crystalline Phase

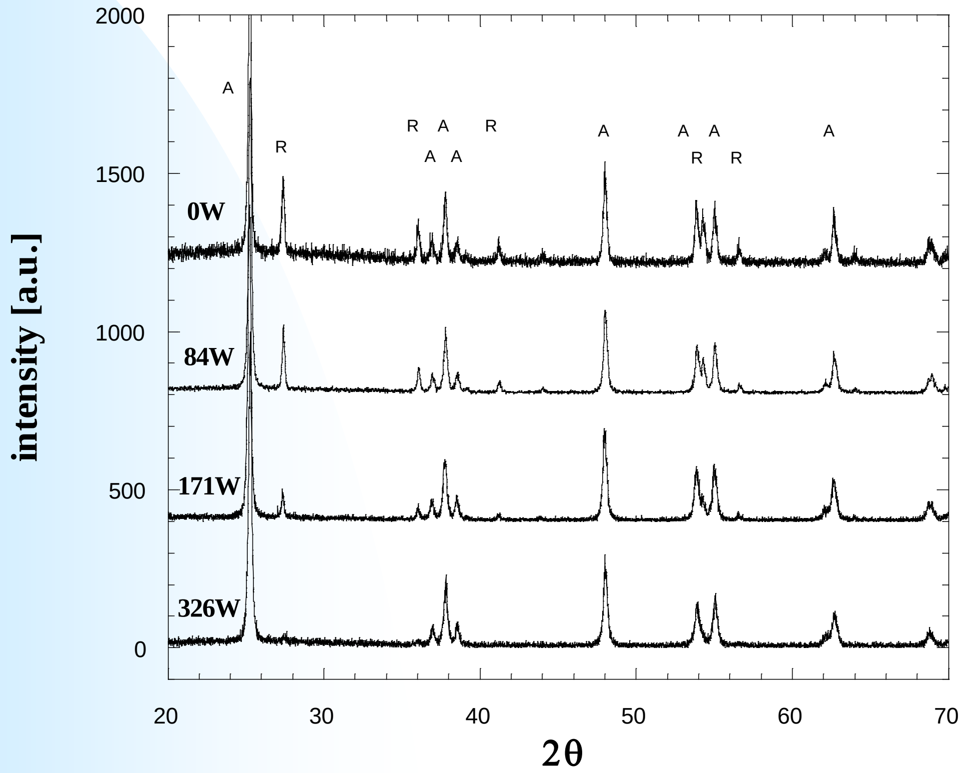

Variations of XRD profiles
; h_L=25mm, h_p=65mm

- Surprising result : thermodynamically stable rutile has been transformed into metastable anatase.

Transformation of Crystalline Phase

(Lee and Choi, 2002 J. Aerosol Science 33, 1-16)

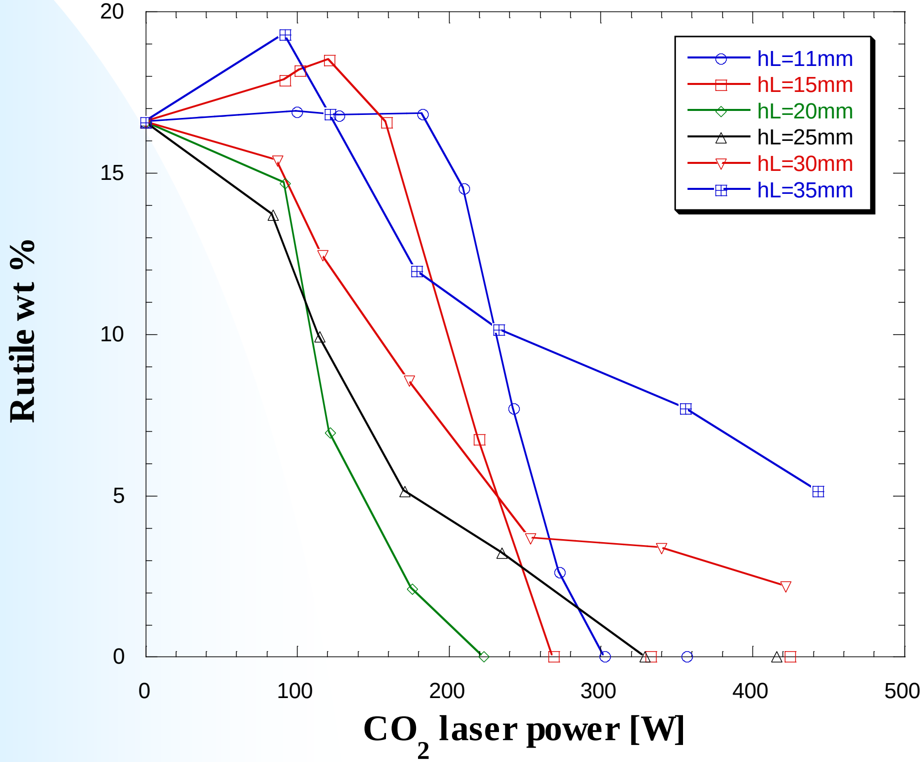

Variations of rutile contents

Laser irradiation in an H2/O2 flame with C2H2 precursor for crystallinity control of carbon nanoparticles

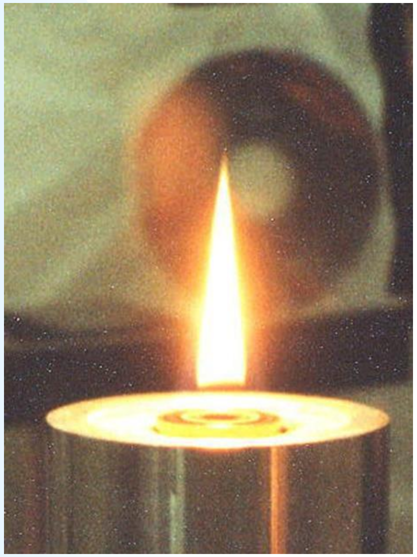

without laser irradiation

800 W

1500 W

TEM images of usual soot and shell shaped carbon particles after laser irradiation at 10 mm

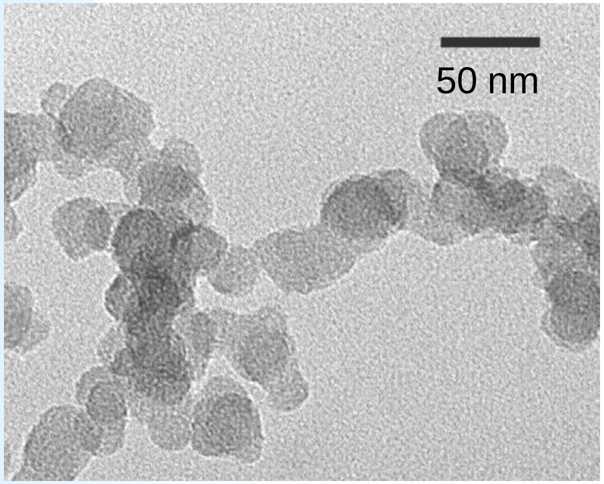

Common Soot

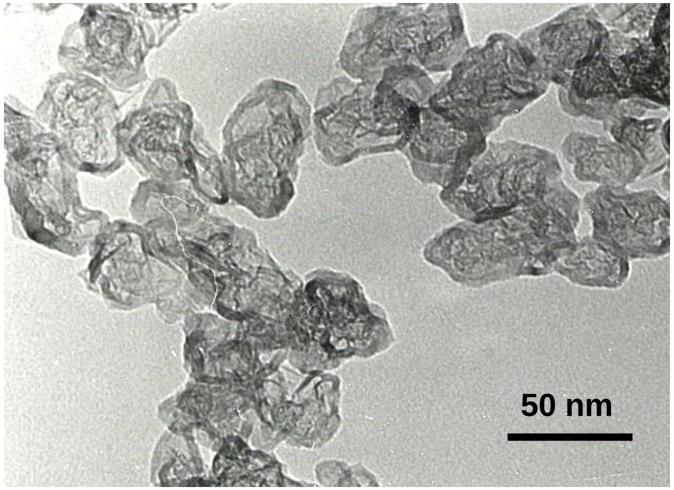

Shell-shaped carbon nanoparticles (SCNP)

Synthesis of shell-shaped carbon nanoparticle(SCNP):

(Choi et al., Advanced Materials, 16, 1721, 2004)

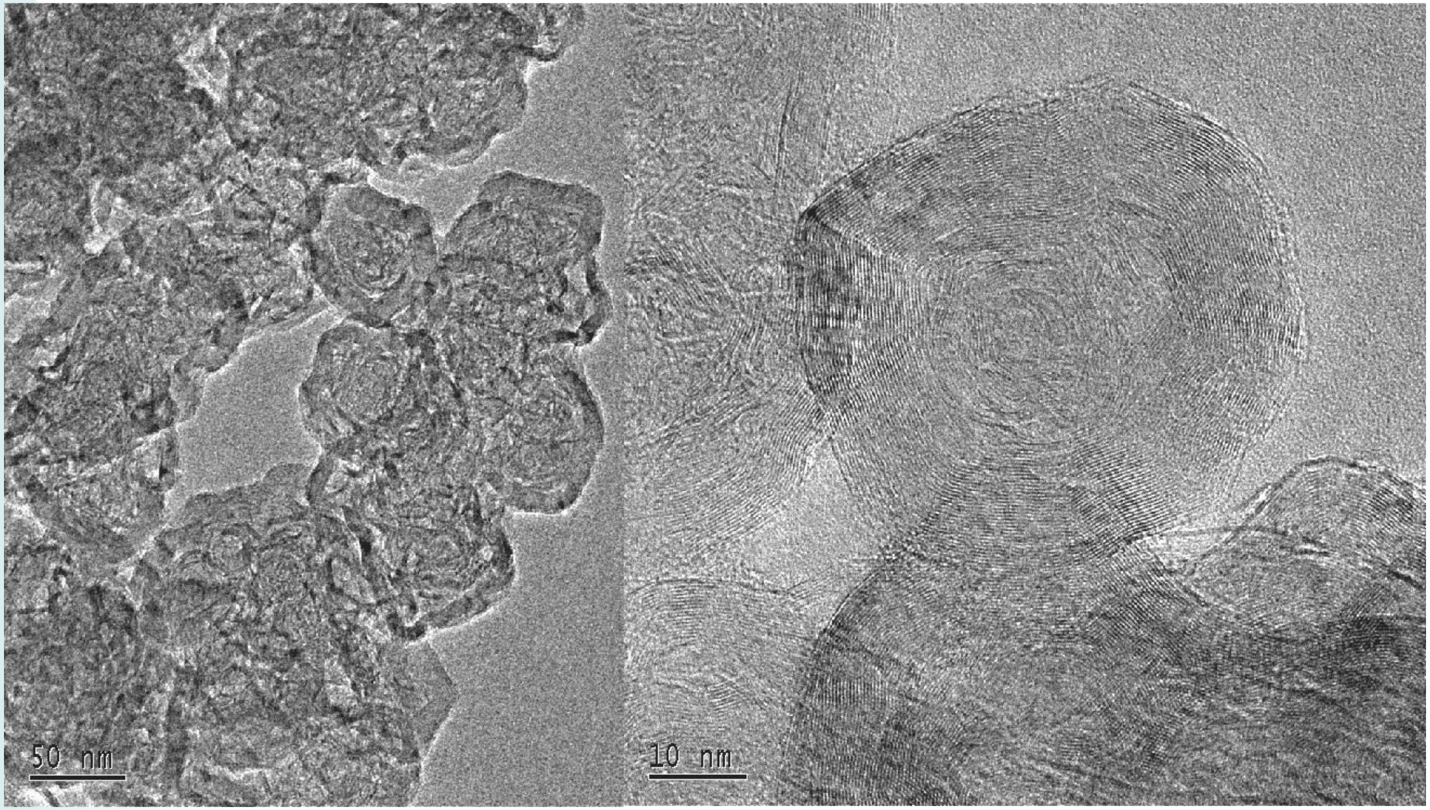

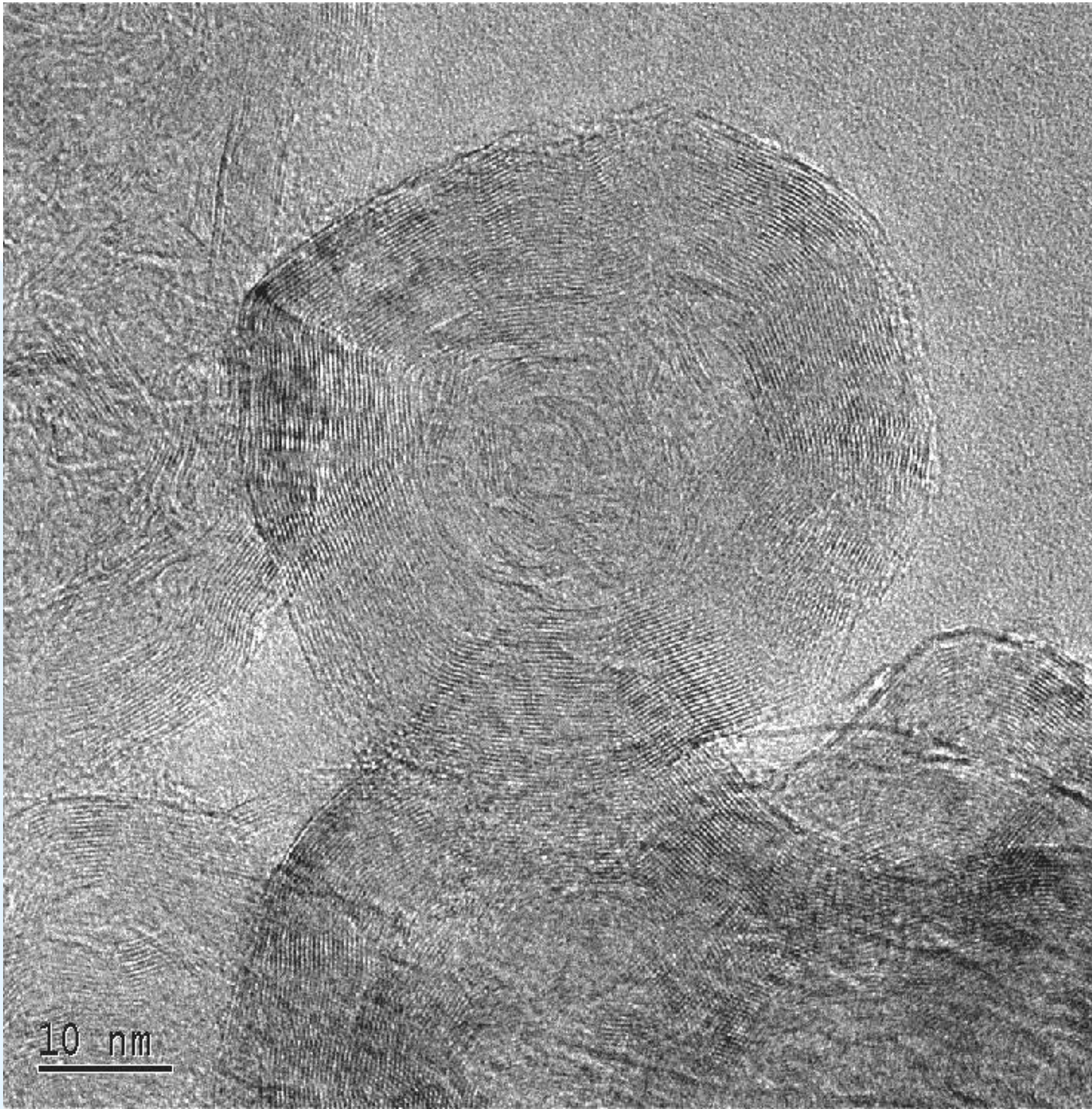

ol

Properties of SCNP

(Advanced Materials, 2004)

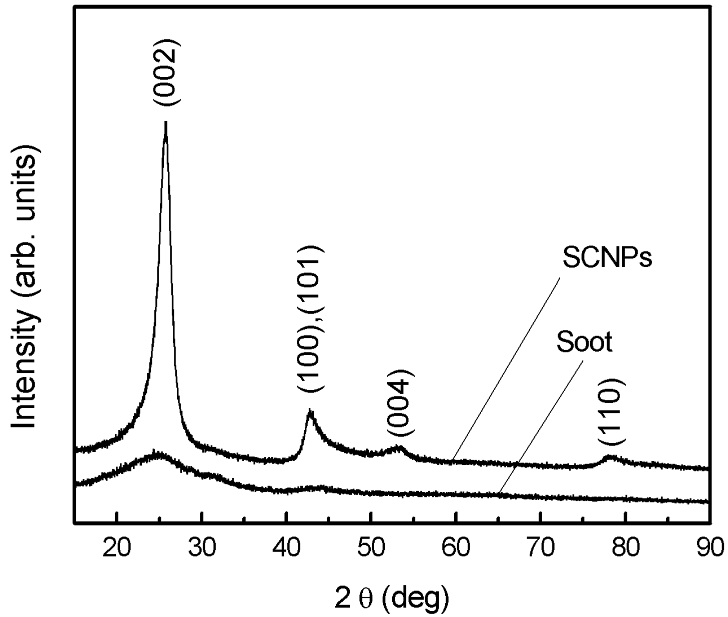

XRD

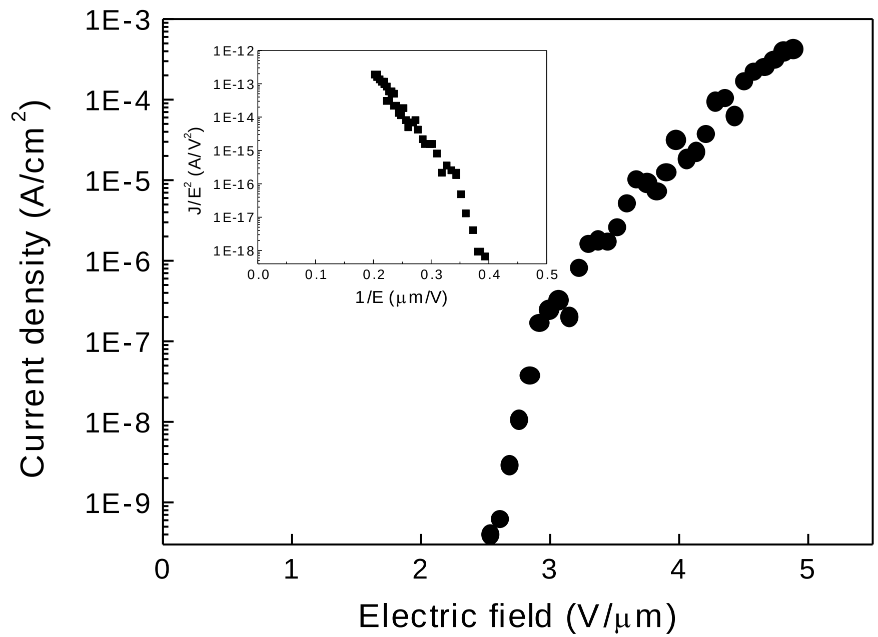

Field Emission Performance

: Comparable to that of Carbon Nanotubes (Applied Physics Letters, 2004, and J. Applied Physics, 2004)